AMERICAN SOCIETY FOR MICROBIOLOGY | Microbiology Spectrum

| Bacteriophages | Research Article

Genomic characterization of *Pseudomonas syringae* pv. *syringae* from Callery pear and the efficiency of associated phages in disease protection

D. Holtappels,[1] S. A. Abelson,[1] S. C. Nouth,[1] G. E. J. Rickus,[1] S. Z. Amare,[1] J. P. Giller,[1] D. Z. Jian,[1] B. Koskella[1,2]

AUTHOR AFFILIATIONS See affiliation list on p. 13.

ABSTRACT The *Pseudomonas syringae* species complex is a heterogeneous group of plant pathogenic bacteria associated with a wide distribution of plant species. Advances in genomics are revealing the complex evolutionary history of this species complex and the wide array of genetic adaptations underpinning their diverse lifestyles. Here, we genomically characterize two *P. syringae* isolates collected from diseased Callery pears (*Pyrus calleryana*) in Berkeley, California in 2019 and 2022. We also isolated a lytic bacteriophage, which we characterized and evaluated for biocontrol efficiency. Using a multilocus sequence analysis and core genome alignment, we classified the *P. syringae* isolates as members of phylogroup 2, related to other strains previously isolated from *Pyrus* and *Prunus*. An analysis of effector proteins demonstrated an evolutionary conservation of effectoromes across isolates classified in PG2 and yet uncovered unique effector profiles for each, including the two newly identified isolates. Whole-genome sequencing of the associated phage uncovered a novel phage genus related to *Pseudomonas syringae* pv. *actinidiae* phage PHB09 and the *Flaumdravirus* genus. Finally, using *in planta* infection assays, we demonstrate that the phage was equally useful in symptom mitigation of immature pear fruit regardless of the Pss strain tested. Overall, this study demonstrates the diversity of *P. syringae* and their viruses associated with ornamental pear trees, posing spill-over risks to commercial pear trees and the possibility of using phages as biocontrol agents to reduce the impact of disease.

IMPORTANCE Global change exacerbates the spread and impact of pathogens, especially in agricultural settings. There is a clear need to better monitor the spread and diversity of plant pathogens, including in potential spillover hosts, and for the development of novel and sustainable control strategies. In this study, we characterize the first described strains of *Pseudomonas syringae* pv. *syringae* isolated from Callery pear in Berkeley, California from diseased tissues in an urban environment. We show that these strains have divergent virulence profiles from previously described strains and that they can cause disease in commercial pears. Additionally, we describe a novel bacteriophage that is associated with these strains and explore its potential to act as a biocontrol agent. Together, the data presented here demonstrate that ornamental pear trees harbor novel *P. syringae* pv. *syringae* isolates that potentially pose a risk to local fruit production, or vice versa—but also provide us with novel associated phages, effective in disease mitigation.

KEYWORDS plant pathogen, phage biocontrol, effectorome, genomic analysis

Pseudomonas syringae comprises a species complex of plant pathogens infecting a wide variety of naturally occurring and agricultural plant species. Currently, more than 60 pathovars are described based on the plant host and disease symptoms (1). Over

Editor Quan Zeng, Connecticut Agricultural Experiment Station, New Haven, Connecticut, USA

Address correspondence to D. Holtappels, d.holtappels@berkeley.edu.

The authors declare no conflict of interest.

See the funding table on p. 13.

Received 14 July 2023
Accepted 11 December 2023
Published 7 February 2024

the past years, "first disease reports" describing strains within the *Pseudomonas syringae* species complex have been outnumbering any other group of bacterial phytopathogens and are comparable to certain fungi (2). Among them, *Pseudomonas syringae* pv. *syringae* (Pss) is considered one of the most generalists due to its ability to infect upward of 180 plant species (3), including multiple *Prunus* species, as well as other stone fruits, mango, citrus, and pear (4–6). Multiple Pss strains have been found to be pesticide resistant over a wide variety of chemical control measures, especially copper. Furthermore, the occurrence of pesticide resistance appears to be positively correlate with the use of the respective pesticide, making diseases caused by this pathogen particularly challenging to control (3, 7, 8).

In pear specifically, Pss is known to cause a disease referred to as blossom blight. The disease mainly manifests early in the growing season and is characterized by blossom and bud blast, shoot dieback, and stem cankers (9). The disease was first reported in 1914 by Barker and Grove in the West of England (10, 11). In 1934, Wilson described the disease for the first time in Californian pear orchards located in the Sierra Nevada foothills (12). Research on a variety of Pss strains collected from pear were characterized by a low cultivar specificity and their ability to cause disease in other plant species such as tomato, underlining the generalist nature of this pathogen (3, 13). In-line with their generalist nature, pathogenic strains of Pss have been found on grasses in infested orchards, creating a reservoir of bacterial inoculum and demonstrating a potential spill-over effect, or vice versa (14). Similarly, the Callery pear (*Pyrus calleryana*), an ornamental pear species originating from Asia that was introduced in the United States in the first half of the 20th century, can act as host to a number of pathogens capable of infecting commercial pears. As these pear trees are susceptible to similar diseases as commercial pear cultivars, such as fire and blossom blight, they pose spill-over risks to spread diseases to commercial and local orchards. Indeed, Pss strain FF5, a common laboratory strain, was initially isolated from Callery pear in Oklahoma, being infectious to both these tree and commercial pears (15).

Recent interest in bacteriophages, viruses of bacteria, as a potential biocontrol measure for bacterial infections in crops has shown promise (16). In the case of Pss specifically, several lytic phages (i.e., those that lyse their host cells) have been described in recent years for use as biocontrol. For example, Pinheiro and colleagues have reported the potential of the commercially available RNA phage ϕ6 to control *P. syringae* pv. *phaseolicola*, *P. syringae* pv. *syringae,* and *P. syringae* pv. *actinidiae* strains based on its stability and microbiological characteristics (17). Another Pss phage, phage SoKa, showed disease control potential in *ex planta* bioassays to reduce symptom development in citrus fruit (5). In sweet cherry, nine phages were reported to reduce disease up to 50% in cherry leaflets (18). Similarly, phage MR8 reduced bacterial population with about three log units in cherry twigs, demonstrating the potential of the phage in biocontrol (6). To date, no phages have been described for use in control of Pss in pear specifically, despite the increasing prevalence of diseases caused by *P. syringae* (2).

To address this research gap, we isolated Pss strains and an associated lytic phage from Callery pear growing in Berkeley, California. We characterized the Pss strains using multilocus sequencing analysis (MLSA) and whole-genome sequencing, placing them within phylogroup 2 of the species complex. Given the limited research on *P. syringae* associated with pear trees, and especially in Callery pear, we hypothesized that the repertoire of encoded effector proteins known to impact pathogen host range and virulence [the effectoromes or effectome (19)] of the isolates collected in this study would differ from other isolated reported in literature. To this end, we performed an *in silico* analysis of the effectoromes of the isolates and compared them to isolates reported in literature. As the disease is manifesting in the phyllosphere, we hypothesized that we would be able to isolate novel phages from diseased leaf samples and that these phages, if amplified and applied to sites of infection, would be able to reduce disease symptoms. We microbiologically and genomically characterized the phages collected

from the phyllosphere and evaluated their biocontrol efficacy against strains collected from Callery pear both *in vitro* and using a detached fruit assay (20–22).

MATERIALS AND METHODS

Bacterium and phage isolations

Diseased leaf samples (black necrotic tissue) were collected from three Callery pear trees (*Pyrus calleryana*) in Berkeley, California in February, March, April, and May 2019 and 2022. The samples (n = 24) were weighed and preserved in a phosphate-glycerol buffer (0.03 M NaH_2PO_4, 0.07 M Na_2HPO_4 $7H_2O$, 1:10 vol% glycerol) at −20°C until further processing. Frozen leaf samples were snap thawed at 56°C and homogenized with a MP FastPrep 24 5G homogenizer using ceramic beads, after which a dilution series was plated on King's Broth (KB) agar plates to isolate single colonies from the culturable fraction of the bacterial community. Plates were incubated for 2 days at 30°C.

To isolate the viral fraction, the homogenate was filtered (0.45 µm) and spotted (5 µL) on a bacterial lawn of the isolated Pss strains. Samples showing lysis zones on the Pss strain isolated from February 2019 were plated in triplicate with double agar to determine the concentration of phage infecting the respective bacterial host per gram of leaf tissue. Plaques were picked with sterile toothpicks, resuspended in a physiological buffer (10 mM TrisHCl), and plated with double agar. This was repeated for three consecutive rounds. Phages were propagated by infecting an exponentially growing culture of the respective host [at an optical density of 600 nm (OD_{600}) of 0.3] in a 1:100 ratio. The coculture was incubated overnight at 30°C and filtered (0.45 µm).

Genomic characterization of *Pseudomonas syringae* pv. *syringae*

Yellow fluorescent bacterial colonies from samples showing blossom blight symptoms were picked, and the bacterial genus was determined by sequencing the 16S rDNA region (27F- AGAGTTTGATCCTGGCTCAG and 1492R- GGTTACCTTGTTACGACTT). Genomic DNA from the isolates reported in this study was isolated using the Qiagen Powersoil Pro Kit as described by the manufacturer and Illumina sequenced at the SeqCenter (Pittsburgh, PA, US). The reads were trimmed with Trimmomatic (v0.38) (23), and the quality was assessed with FastQC (v0.11.9). Trimmed reads were assembled with Unicycler (v0.5.0) (24) to obtain draft genomes and annotated using Prokka (v1.14.6) (25). A multilocus sequencing analysis was performed based on the concatenated gyrB and rpoD sequences (3) that were bioinformatically extracted from the bacterial genomes and based on sequences reported in literature using MEGA11 (v11.0.11) (26). Sequences were aligned with MUSCLE, followed by constructing a neighbor-joining tree with 1,000 bootstraps and visualized with iTol (v6.6) (27).

A core genome analysis was built by extracting *Pseudomonas syringae* genomes from NCBI (December 2022, Table S1). The quality of the assemblies was evaluated using BUSCO, and genomes of a score above 0.95 were selected for downstream analysis. An ANI analysis was performed by means of fastANI (v1.33) (28). The core genome was determined using Ppanggolin (v.1.2.74) (29), and a phylogenetic tree was constructed using FastTree (30) with default parameters. Similarly, the effector analysis was performed using the effector database from Dillon et al. (31). In short, a Blastp analysis was conducted on strains closely related to Pss11.5 and Pss16QsV supplemented with strains originating from pear (FF5, B301D, B301D-R, and LMG5084) with a threshold of 50% query coverage and an *e*-value of 1e−20 to ensure a conservative annotation of putative effector proteins. Additionally, the protein sequences were manually curated to limit the number of false positives in the data set. An absence-presence matrix for all the different effectors was built and analyzed using the JMP Pro 16 software by a default hierarchical clustering method.

Phage characterization

The lysis of an exponentially growing culture of Pss 16QsV (OD_{600} at 0.1) was followed over time after infecting the culture with different multiplicities of infection (MOI of 0.1–1–10) in sixfold using an Infinite M nano Tecan plate reader. The adsorption kinetics of the phage on each of two Pss strains were assessed by infecting a culture at exponential growth phase (OD_{600} of 0.3) with an MOI of 0.01. Samples were taken directly after, and then 10 minutes after, inoculation and treated with chloroform, to kill bacterial cells and halt any active phage replication. Phage particles were enumerated using a double agar overlay, and the number of free phage (PFUs; plaque forming units) was calculated. The adsorption constant was determined according to Hyman and Abedon (32).

Phage genomic DNA was extracted by means of a phenol/chloroform/isoamyl alcohol extraction and purified using an ethanol precipitation. The genomic DNA was Illumina sequenced (The SeqCenter, Pittsburgh, PA), and reads were trimmed as processed as described above. Assembled contigs were automatically annotated using the Phage algorithm of the PATRICBRC server (33) and manually curated. We taxonomically classified the phage using the VipTree server (34) and VIRIDIC (35). Genome maps were generated with EasyFig (36). The genome of phage 16Q is available at NCBI with accession number OR001909.

Ex planta bioassay for assessing the potential of phage 16Q as a biocontrol agent

Pathogenicity of the isolated *Pss* strains and biocontrol potential of the phage were assessed using two unripe pear assays (20–22, 37). In the first assay, unripe pears were collected from the University of California Gill Tract Community Farm and surface sterilized by submerging them in 1% bleach for 5 minutes followed by three rinses with sterile mQ water. Afterward, the pears were washed with 70% ethanol and dried in a laminar flow. Pss strains were grown in liquid KB medium, centrifuged at 4,000 *g* at 4°C, and resuspended in phosphate-buffered saline (PBS). The fruits were pierced with sterile toothpicks and inoculated with 10^8 CFU/mL (5 µL) of bacterial suspension at the site of injury across three replicates per pear. Negative controls were inoculated with PBS buffer. The efficiency and local adaptation (i.e., whether phages were more infective to strains collected from the same tree in the same year) of the phages were assessed by adding 5 µL of phage suspension (10^8 and 10^9 PFU/mL) prior to inoculating the bacteria (10^8 CFU/mL) in triplicate. The pears were incubated for 5 days at 30°C in sterile plastic containers. The second immature pear assay was performed similarly to the first assay with immature fruit from Asian pear (*Pyrus pyrifolia*) collected from UC Davis. In total, six immature pear fruits were inoculated per condition with a single inoculation site per pear. Inoculated pears were incubated for 6 days at 30°C in closed plastic containers to maintain the humidity. The surface of the diseased area was measured using Fiji (38). An analysis of variance (ANOVA) model considering random effects for individual pears was used to determine the effect of phage treatment on disease outcome using the JMP pro 16 software.

RESULTS

Ornamental Callery pear trees in Berkeley suffer from blossom blight caused by *Pseudomonas syringae* pv. *syringae* as confirmed by an MLSA and core genome alignment

Diseased samples from Callery pear trees (Fig. S1) collected from March 2019 and March 2022 showed the presence of *Pseudomonas*-like colonies when plated on KB medium that were confirmed to be *Pseudomonads* by sequencing of the 16S region. A multilocus sequencing analysis based on the gyrB and rpoD gene sequence, according to Guttierez-Barnanquero and colleagues, demonstrated that indeed the two strains cluster together with other *Pseudomonas syringae* pv. *syringae* strains within phylogroup 2 (Fig. 1) (1, 3). As such, our analysis confirmed the presence of Pss in Callery pear in the city

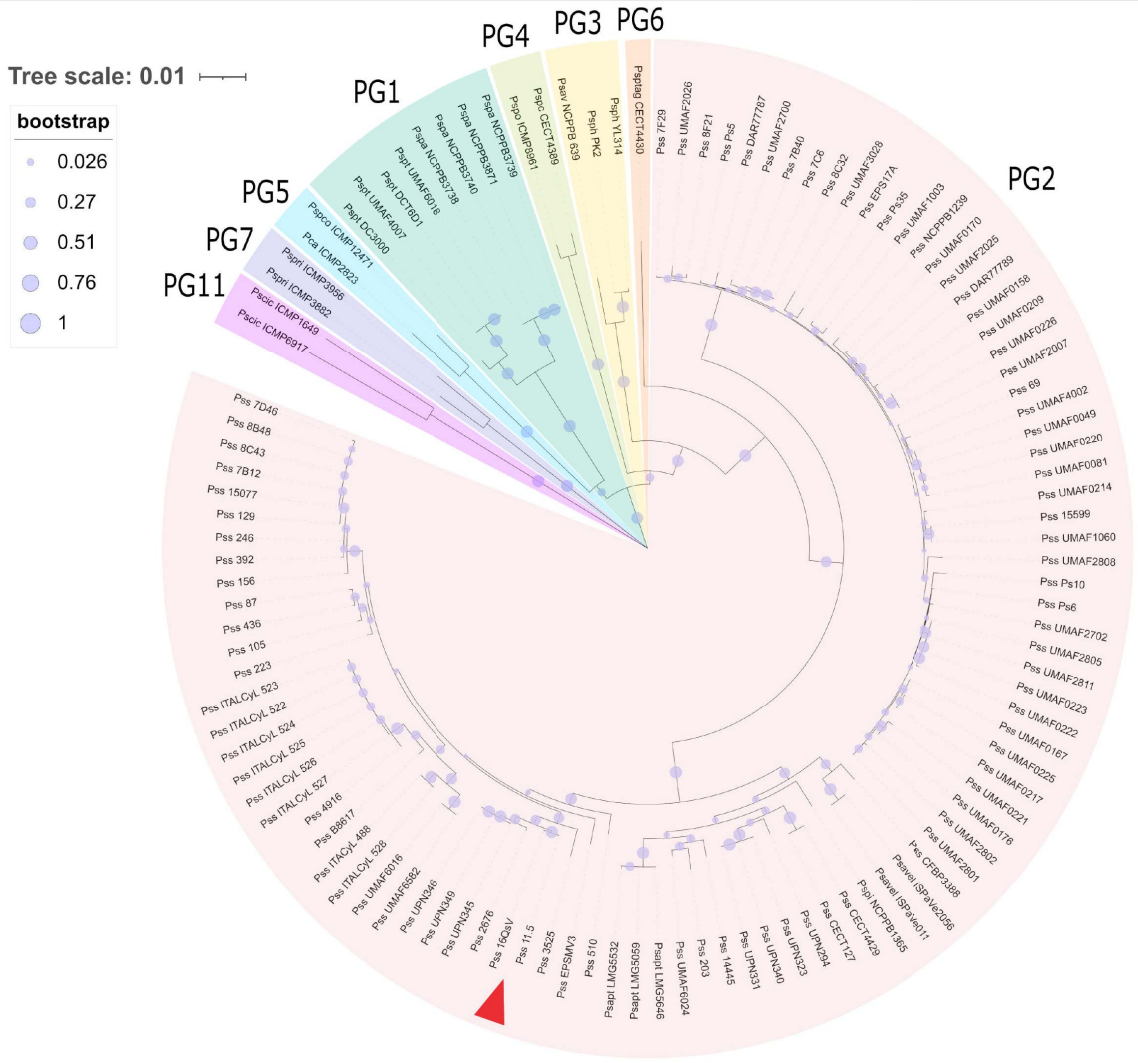

FIG 1 Multilocus sequence analysis of *Pseudomonas syringae* strains according to Gutierrez-Barnanquero et al., including phylogroups 1, 2, 3, 4, 5, 6, 7, and 11 as outgroup. The neighbor-joining tree (1,000 bootstraps) was constructed based on an alignment of partial gyrB and rpoD sequences. The bootstrap values are shown on every node as proportional circles. The evolutionary distance is shown in units of nucleotide substitution per site. The different phylogroups are shown as follows: phylogroup 1 (PG1) in teal, phylogroup 2 (PG2) in red, phylogroup 3 (PG3) in yellow, phylogroup 4 (PG4) in green, phylogroup 5 (PG5) in blue, phylogroup 6 (PG6) in orange, phylogroup 7 (PG7) in purple, and phylogroup 11 (PG11) in violet. Pss strains Pss16QsV and Pss11.5 cluster together within PG2 (indicated with red arrow). The phylogenetic tree was generated with MEGA11 and visualized with iTol.

of Berkeley (CA), and hence, the disease blossom blight. Based on this phylogenetic analysis, Pss16QsV (collected in March 2019) and Pss11.5 (collected in March 2022) were most closely related to Pss2676, PssUNP345, PssUNP349, and PssUNP346, all isolated from bean, emphasizing the generalist nature of Pss phylogroup 2. When only considering those strains collected from pear, Pss16QsV and Pss11.5 were most closely related to Pss7D46, Pss8B48, Pss8C43, Pss7B12, and PssEPSMV3. Other isolates collected from pear trees included in this analysis clustered together in a separate subcluster within phylogroup 2, underscoring the diversity of this specific phylogroup.

A more in-depth analysis of the genomic diversity of the isolated strains was conducted. To this end, over 600 draft genomes were extracted from NCBI and analyzed for their completeness using BUSCO. Genomes with a completeness over 95% were used to characterize the pangenome and determine the core genome (n = 485). Based on ANI, we identified that our isolates Pss11.5 and Pss16QsV share at least 95% nucleotide identity with other members of PG2, except strain 642 with which our strains share 94%

(Table S2). According to our pangenome analysis, the pangenome of *P. syringae* consisted of 2,606,355 genes grouped in a total of 73,863 gene families. From these families, 2,637 were persistent gene families (shared between 90% and 100%), 8,470 were shell gene families (shared between 15% and 90% of genomes), and 62,756 were cloud gene families (shared <15% of genomes). Figure 2 shows a phylogenetic tree based on the persistent gene families. Similar to our MLSA, a grouping of the genomes was observed that resembled the different phylogroups as defined for the species of *P. syringae* as reported previously (31). The strains collected in this study clustered together with other strains defined as members of phylogroup 2, further confirming the results obtained from our MLSA.

Pss16QsV and Pss11.5 both have a total genome size of 5.87 Mbp. Based on their core genome, Pss16QsV and Pss11.5 were most closely related to CFBP4215, PssA1M163, NRS 2339, and NRS 2340 (all over 98% ANI). All of these strains originated from *Prunus avium* (sweet cherry), except NRS 2340 which was originally isolated from pear (*Pyrus* sp.) (39).

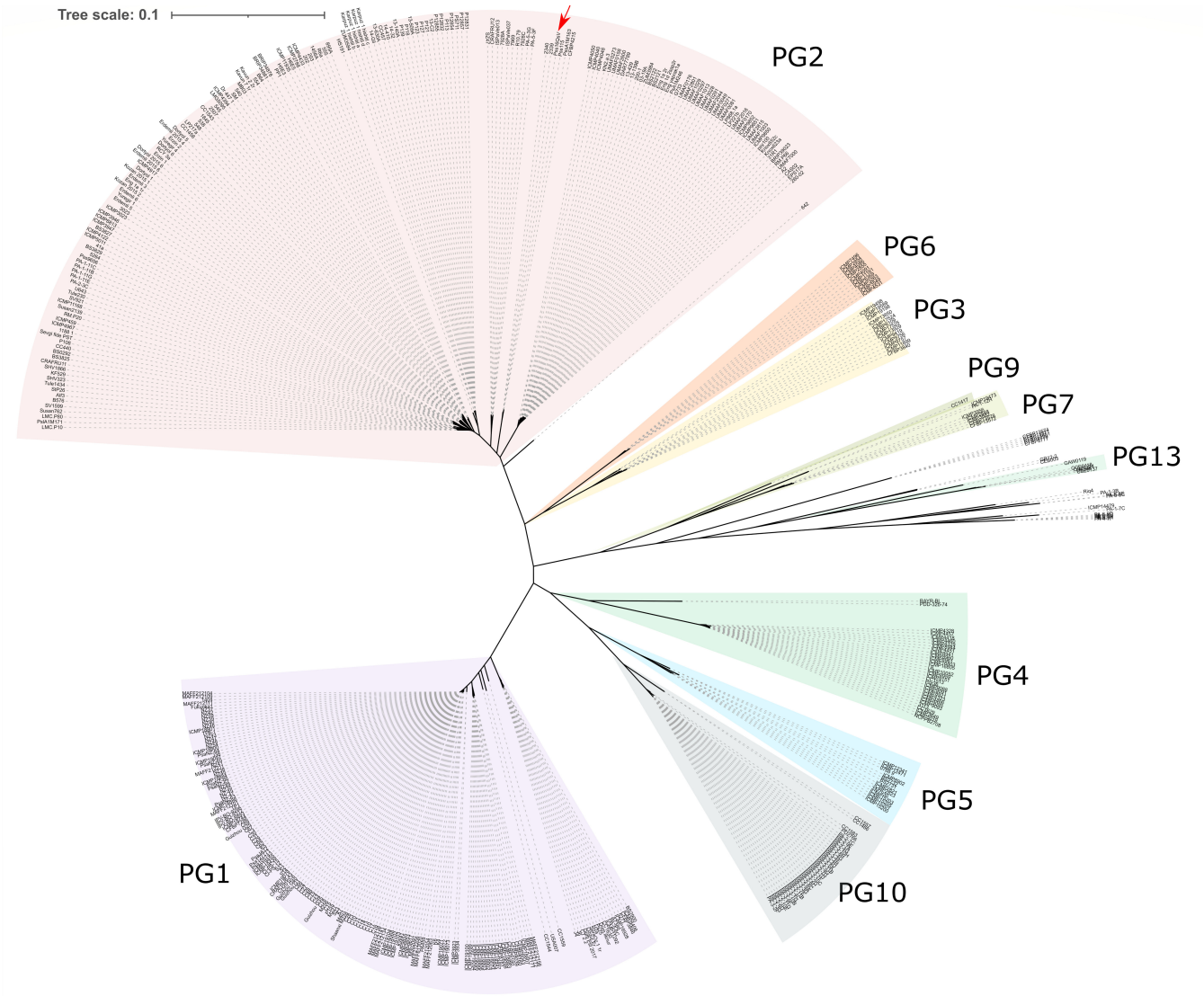

FIG 2 Unrooted phylogenetic tree (n = 485 isolates) based on an alignment of the persistent gene families within *P. syringae*. Based on their phylogenetic distance, isolates cluster together according to their phylogroup (purple is phylogroup 1 PG1, pink is phylogroup 2 PG2, orange is phylogroup 6 PG6, yellow is phylogroup 3 PG3, olive green is phylogroup 9 PG9, green is phylogroup 7 PG7, teal is phylogroup 13 PG13, dark teal is phylogroup 4 PG4, blue is phylogroup 5 PG5, and gray is phylogroup 10 PG10). Strains Pss16QsV and Pss11.5 are indicated with a red arrow.

Effectoromes are non-random within the phylogeny of *P. syringae,* and Pss16QsV and Pss11.5 encode effector proteins unique for their clade

Effector proteins are considered one of the main virulence factors of *P. syringae*. Hence, we mined the genomes of the closest relatives (n = 100) of Pss16QsV and Pss11.5 supplemented with other strains isolated from pear (FF5, B301D, B301D-R, and LMG5084). According to our conservative bioinformatical pipeline, the isolates had on average 18 effector proteins encoded in their genomes, ranging from a low of 11 (Pss FF5—isolated from *Pyrus calleryana*) to a high 27 (strain 203—isolated from *Pisum sativum*). Pss16QsV, Pss11.5, and LMG5084 (*Pyrus communis*) were each annotated to encode 16 effector proteins in their genomes, which is higher compared to other strains isolated from pear with an average of 14.6 effector proteins encoded (±1.8). Interestingly, our analyses pointed out that *P. syringae* collected from *Malus* encoded on average 23 effectors (±5). Our overall analysis on the effectoromes of PG2 *P. syringae* isolates showed that all strains encoded HopAA1, HopAG1, HopAH1, HopB4, and HopM-ShcM1. Most strains carried the genes for HopI1 and HopB2, but HopI1 was not predicted in strains FF5, 13-630A, and 14-Gil, while HopB2 was not encoded by ISPaVe037, LP686.1a, and PA-5-3G. Interestingly, our analysis could not detect *avrE1* in Pss FF5, while the gene was present in all other strains. HopAM1 and HopZ6, on the contrary, were only encoded by strains PP1 and HS191, respectively.

We clustered the strains according to the absence and presence of the effector proteins by means of hierarchical clustering (Fig. 3A). Based on this clustering method, seven different groups were distinguished. Comparing the phylogeny of these strains and their effectorome, clade 1 only contained isolates previously classified as PG2 clade 4. Similarly, group 2 and group 3 included primarily isolates from PG2 clade 1, with strain SZ47 as an exception. Group 4, containing isolates Pss11.5 and Pss16QsV, consisted of PG2 clade 2. Group 5 was mainly composed of strains from PG2 clade 4, and groups 6 and 7 included isolates from PG2 clades 4 and 1, respectively. As such, our analysis demonstrated a clear relationship between the different clades within PG2 and their effectorome. Indeed, an analysis of similarities showed significance between the effectorome of the clades within PG2 (R = 0.614, P-value = 0.001), suggesting that effectoromes are not random within the different clades of PG2 and that there is an association between phylogeny and the effectorome. Within these groups, however, there were individual genes detected in isolates that are unique to the overall pattern, demonstrating a gain and loss of individual effector genes and, hence, plasticity in the effectorome.

Similar to our phylogenetic analysis, Pss16QsV and Pss11.5 clustered together with CFBP4215, NRS 2339, and NRS 2340, further underlining the close evolutionary relatedness between these strains and the non-randomness of the effectorome. Remarkably, other isolates collected from pear, B301D, B301D-R, and LMG5084 clustered within this group but not FF5. All strains within group 4 were predicted to encode HopAL1, unique for cluster 3 and cluster 6.

Next, we looked more closely at isolates collected from *Rosaceae* species and found a clear conservation of effector proteins (Fig. 3B). We hypothesize that these proteins are essential for *P. syringae*'s association to plants within the Rosaceae family. Yet, we observed some key differences in the effector profiles. Pss11.5 and Pss16QsV, for example, were predicted to encode AvrRpm1 unique for all strains originating from *Rosaceae*. Similarly, strain 2340 was the only pear-associated isolate encoding HopAB1. The effector profile of Pss strain FF5 was remarkably distinct from the other strains assessed comprising HopBF1.

Novel lytic Pss phage 16Q infects both Pss16QsV and Pss11.5 with similar efficiency and represents a novel phage genus

In addition to the bacteria, we isolated four bacteriophages that were capable of infecting (i.e., forming plaques on a lawn of) strain Pss16QsV from the February (sympatric), March, April, and May 2019 samples. Upon sequencing the phage genomes,

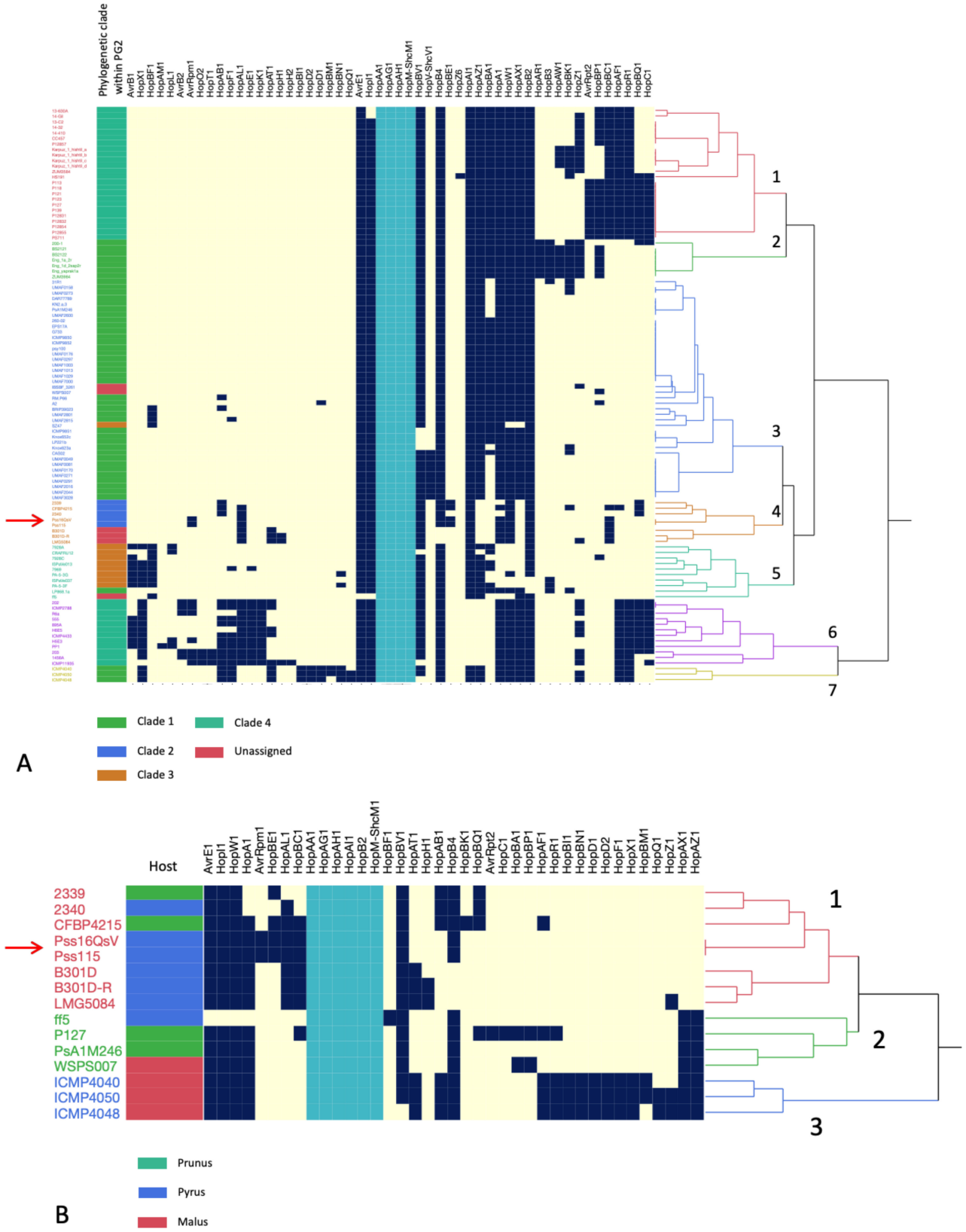

FIG 3 Absence-presence matrix and hierarchical clustering of the screened effector proteins within the different Pss isolates. Yellow indicates if the gene encoding the specific effector protein is not present, dark blue if the gene is encoded in the genome. Strains collected in this research are indicated with a red arrow. Effectors that are encoded by all strains are indicated in light blue. (A) The effectorome of a subset of the PG2 strains classified according to our ANI and

(Continued on next page)

FIG 3 (Continued)

core genome analysis supplemented with strains specifically isolated from pear (in green clade 1, in blue clade 2, in brown clade 3, in teal clade 4, and in red the unassigned isolates). Based on the absence/presence of the effectors, seven groups can be distinguished (red, green, blue, orange, teal, and purple). All strains encode HopAA1, HopAG1, HopAH1, HopB4, and HopM-ShcM1. On average, the different strains encode 18 effector proteins. (B) In detail, the effectorome of Pss isolates isolated from *Rosaceae* trees (in green *Prunus*, in blue *Pyrus*, and in red *Malus*). Within these strains, three different patterns were determined based on the absence and presence of specific effector proteins.

we could not identify single-nucleotide polymorphisms or other signs of genome plasticity across the phage genomes. As such, we continued our phage characterization with phage 16Q (February 2019), collected in the same sample as Pss16QsV. We evaluated the infection efficiency of the phage in liquid broth on both Pss16QsV (sympatric strain) and Pss11.5 (allopatric strain from a different tree and collected in 2022; Fig. S2). This analysis demonstrated that Pss16QsV and Pss11.5 are equally susceptible to phage 16Q in liquid broth. Additionally, we evaluated the adsorption kinetics of phage 16Q on both the sympatric and allopatric strain but found no significant difference in the adsorption of 16Q between the two combinations (Fig. S3). The adsorption constant for 16Q on both Pss16QsV and Pss11.5 was 7.12e−6 mL/min after 10 minutes, suggesting a rather inefficient adsorption of phage 16Q to both hosts.

The genome of 16Q is 94.6 kb with a GC content of 45%. Based on our annotation of the 16Q genome, the phage encoded a panel of 15 tRNAs. Yet, no signs of alternative coding density were detected based on the coding density in alternative translation tables (4, 11, and 15) (40). A phylogenetic analysis of the 16Q genome revealed that this phage is related to the *Pakpunavirus, Otagovirus,* and *Flaumdravirus* genus (VipTree analysis—Fig. S4). A more detailed study of the sequence identity between these genera showed that phage 16Q shares over 35% sequence identity with the *Otagovirus* and *Flaumdravirus* genera (Fig. 4A). Interestingly, all representative members as currently described in the taxonomy database from the International Committee on Taxonomy of Viruses (ICTV—December 2022) infect *P. syringae*, emphasizing their relatively close relatedness and a recent common ancestor. Furthermore, the *Otagovirus* and *Flaumdravirus* genera shared about 10% sequence identity with the *Pakpunavirus* genus which is primarily represented by *P. aeruginosa* phages (ICTV—December 2022), again illustrating the relatedness, evolutionary trajectory, and phage-host association. Phage 16Q shared 66.74% identity with its closest neighbor, *P. syringae* pv. *actinidiae* (Psa) phage PHB09. Based on the threshold of sequence identity between phage genera as determined by the ICTV (41), we suggest that phage 16Q represents a new phage genus, closely related to Psa phage PHB09 and the *Flaumdravirus* genus.

This relatedness was further highlighted by comparing the genomes of phage 16Q, *P. syringae* pv. *porri* (Pspo) phage KIL5, and Psa phage PHB09 (Fig. 4B). Here, we observed a conservation of genome architecture among the different phages. Similarly, Pspo phage KIL5 and Psa phage PHB09 encoded no genes related to a temperate lifestyle, and no bacterial virulence-associated genes were identified in the genome, suggesting a strictly lytic lifestyle of 16Q and the phage's potential as a biocontrol agent [i.e., low probability of mediating horizontal gene transfer (HGT) during genome integration].

The application of phage 16Q causes a significant disease reduction as determined by an *ex planta* bioassay in immature pear fruit

We evaluated the efficiency of phage 16Q in disease protection of both a sympatric and allopatric phage-bacterium combination based on an immature fruit assay (Fig. S5 and S6). We found a clear significant increase in the log-transformed diameter of the necrotic tissue when the pear fruits were inoculated with Pss (ANOVA, *P*-value of <0.0001); however, there was no significant difference in the diameter of the necrotic tissue between Pss16QsV and Pss11.5. This suggests that both strains caused similar disease symptoms. When the pear fruits were pretreated with phage, there was a significant reduction of the necrotic tissue developed (*P*-value of <0.0001). The other main effect in the model was the multiplicity in infection (or ratio of phage to bacterium), which

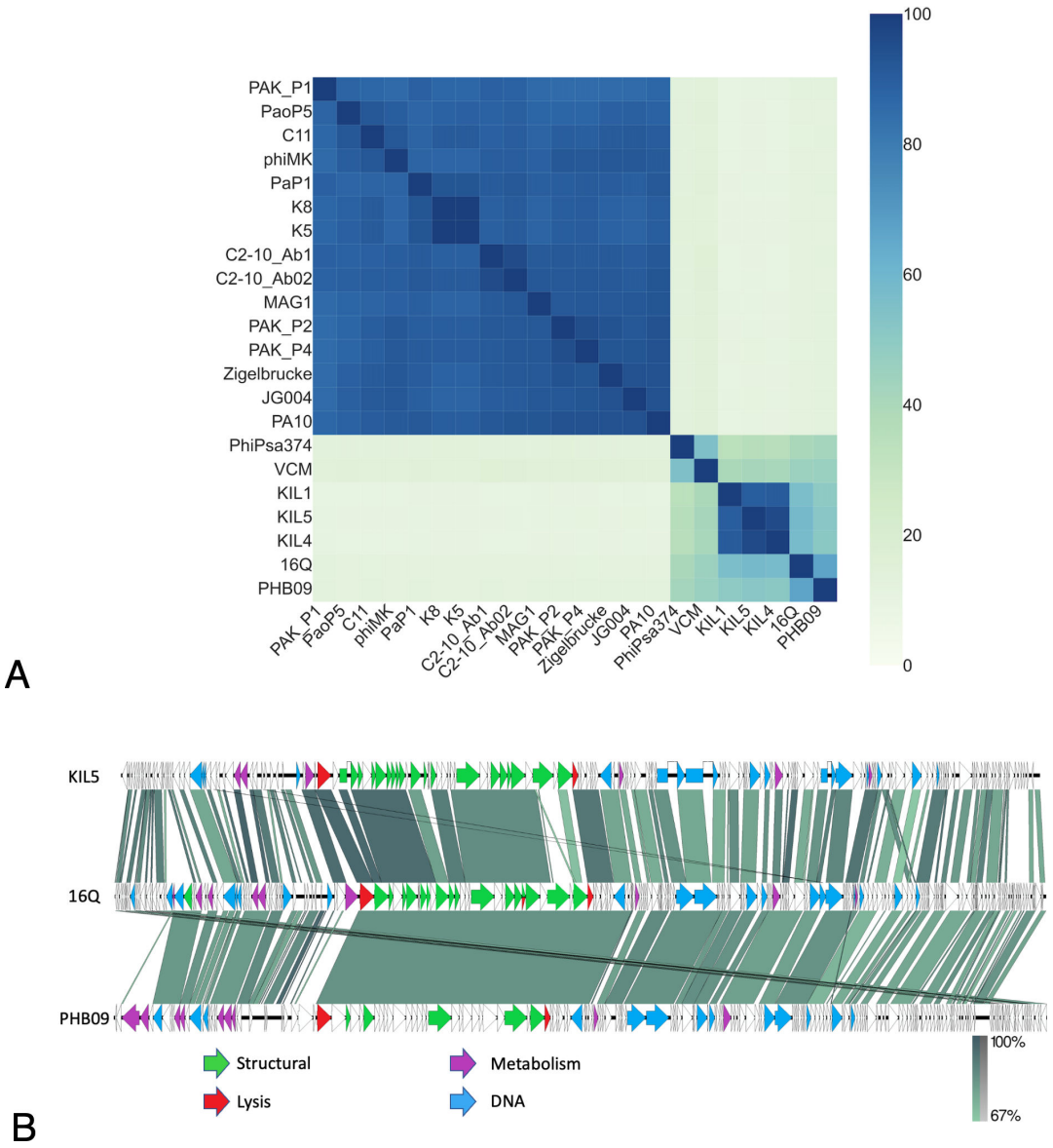

FIG 4 (A) Heatmap of a VIRIDIC analysis of phage 16Q along with members of the *Pakpunavirus, Flaumdravirus,* and *Otagovirus* genera as identified as the closest relatives of phage 16Q based on a VipTree analysis of the 16Q genome. Pss phage 16Q shares 66.74% sequence identity with its closest neighbor *Pseudomonas syringae* pv. *actinidae* phage PHB09 and between 56% and 58% with members of the *Flaumdravirus* genus *Pseudomonas syringae* pv. *porri* phages KIL1, KIL4, and KIL5. (B) Genome maps of Pspo phage KIL5, Pss phage 16Q, and Psa phage PHB09. The phages share a similar genome architecture and homology (blastn) between the different gene clusters. Genes coding for DNA-associated proteins are shown in blue, structural proteins in green, lysis associated in red, and metabolism associated in violet. Genome orientation and ends of phage 16Q were aligned with Pspo phage KIL5 as these were experimentally determined using primer walking (42) .

was not significant, suggesting that both treatments worked equally well. Similar results were obtained when individual treatments were evaluated against each other using a Tukey-Kramer honestly significant difference (HSD) test correcting for multiple comparisons (connecting letters in Fig. S7). Here, there was no significant difference between the two strains, yet there was a significant effect of the phage treatment. This suggests that there was no significant effect of local adaptation of phage 16Q in reducing symptoms by either of the two strains.

Our results were further confirmed in a second immature pear assay with immature Asian pear fruits (*Pyrus pyrifolia*). In this assay, we found a significant reduction of

the necrotic tissue between phage treated and non-phage treated (ANOVA, *P*-value = 0.0095). Evaluating the individual treatments against each other correcting for multiple comparisons (Tukey-Kramer HSD test), we found a significant difference between the positive controls and fruits treated with a 10-fold higher phage concentration, illustrating that this concentration is desirable for disease prevention (as illustrated by the connecting letters report on Fig. 5). Our results showed that in two independent assays with different pear varieties, our phages were able to prevent disease and that a 10-fold higher concentration of phage compared to bacteria performed well in both assays to mitigate necrosis.

DISCUSSION

Pseudomonas syringae is a widespread pathogen impacting multiple important crops around the world. In this study, we report and characterize two strains of Pss collected from Callery pear trees exhibiting necrotic symptoms in Berkeley, California. Our immature fruit assays demonstrate that these isolated strains cause disease symptoms in pear, confirming the presence of virulent Pss strains resulting in blossom blight. This was further validated via an MLSA and whole-genome sequencing which demonstrate close phylogenetic relatedness with other isolates classified as Pss phylogroup 2. Isolates within this phylogroup are described to infect a wide array of plant species (2, 43). A recent ANI analysis of 99 draft and complete Pss genomes showed that there are 3 clades within PG2 sharing at least 95% nucleotide identity (44). Our re-analysis of these same isolates confirms these results, but including more strains in the analysis reveals the existence of a fourth clade within PG2, indicating that we are only beginning to discover the complex evolutionary history of this phylogroup. On average, we demonstrate that over the whole species complex of *P. syringae,* there is a large portion of accessory gene families. This could be explained by the diverse lifestyles and host associations of isolates

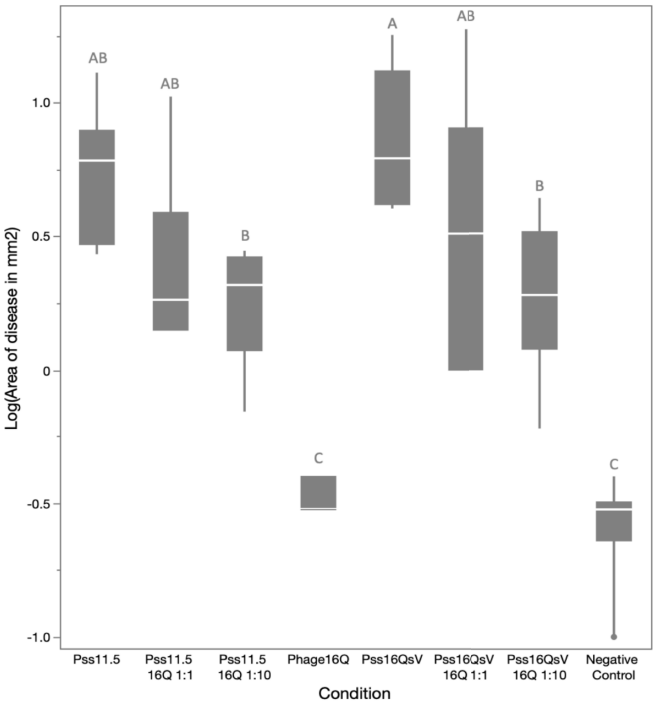

FIG 5 Quantile boxplots of the logarithmic area of necrotic tissue (mm^2) around the inoculation sites in immature pear fruits (n = 9). Pss16QsV and Pss11.5 were inoculated with a concentration of 10^8 CFU/mL as well as phage 16Q at a ratio of 1:0 (MOI 0—no phage), 1:1 (MOI 1), and 1:10 (MOI 10). As negative control, pears were inoculated with PBS. Letters A–B represent different groups of significance (Tukey-Kramer HSD test for multiple comparison, *P*-value <0.05).

within the species complex and the genetic background necessary to support these diverse lifestyles (31, 45).

Essential to the lifestyle of many *P. syringae* isolates are effector proteins. Type III secreted effector proteins, known as the effectorome, are essential in mediating host-microbe interactions, as these proteins are translocated to the host cytoplasm where they influence a various cellular processes resulting in host takeover (46). Currently, over 66 families of effector proteins are described for *P. syringae*, demonstrating the diverse strategies that this bacterial species has developed over the course of evolution (31). A conservative screening of the presence/absence of specific effector proteins in the genomes of 494 strains gave clear insights into the number of effector proteins encoded by different phylogroups, with members of PG2 having a median effector count of 18 effectors per genome (31, 47). The 2 additional strains reported in this study encode only 16 effector proteins, but this number is higher compared to other isolates from pear specifically (average of 14.6 ± 1.8). Remarkably, we find two effector proteins that are encoded by all strains, including these new isolates. Our analysis demonstrated that HopAH and HopAG are encoded by all PG2 isolates, in-line with previous evidence for conservation of these effectors within PG2 (31, 44). Indeed, AvrE, HopM, HopAA, and HopB are known to be part of the conserved effector locus (31, 46, 48). We further show that there is more similarity between clades within PG2 than there is among clades, suggesting evolutionary conservation of effector proteins. Despite this, there is quite some variability in the effectoromes of the different strains, underlining the role of horizontal gene transfer of effector genes and the evolutionary arms race between *P. syringae* and its plant hosts (46, 49). Indeed, HGT plays an important role in the acquisition of effector proteins (50). The genes *hopBB1* and *hopBF1* were, for example, shown to be embedded on plasmids in cherry-pathogenic isolated. Moreover, *hopAR1* was encoded by prophages, suggesting that effectors are acquired through a myriad of HGT strategies (51).

A potential strategy for limiting the spread and impact of Pss is by developing a sustainable biocontrol strategy to contain the disease. To this end, we isolated novel bacteriophages from diseased samples infecting the strains collected from Callery pear. We found one phage (16Q) multiple times (across different trees and collection months), suggesting a widespread distribution of this phage. The genomic analysis of the phage genome revealed that it encodes 15 tRNAs in its genome, making the phage quite independent from its host for translation. This raises the hypothesis that phage 16Q efficiently synchronizes its own transcription and translation, which has been hypothesized to be of great importance for efficient host takeover (52, 53). Our phylogenetic analysis of phage 16Q demonstrates a relatedness to other *Pseudomonas* phages, members of the *Pakpunavirus, Otagovirus,* and *Flaumdravirus* genera (Fig. 3). The former primarily consists of *Pseudomonas aeruginosa* phages, while the latter two comprise *P. syringae* phages. Interestingly, the overall diversity among phages infecting *P. aeruginosa* is lower than that among phages of *P. syringae*, which corresponds to previous findings of higher diversity among *P. syringae* isolates compared to *P. aeruginosa* strains (54). Remarkably, all seven *P. syringae* phages within the same subcluster as 16Q were reported to be suitable candidates for biocontrol. For example, *P. syringae* pv. *actinidiae* phage PhiPsa374 was shown to be stable in storage and did not show any signs of transduction nor a temperate lifestyle. Additionally, this phage had a broad host range, infecting multiple Psa strains within the tested collection (55). A more detailed analysis from Warring and colleagues on this phage species demonstrated their effectiveness, both *in vitro* and *in vivo* (56). They found that the phages adsorbed to lipopolysaccharide residues on the Psa cell surface both *in vitro* and *in planta,* and significantly reduced the bacterial load *in planta*. Our immature pear assay demonstrated a similarly significant effect of disease mitigation after administering phages, comparable to Pss phage SoKa in citrus (5). Our study further emphasizes the ability of phages to be used as biocontrol agents to reduce the effects of disease in crops as comprehensively reviewed elsewhere (57, 58)

One aspect often overlooked when designing phage therapies is the source of the phage and whether it comes from the same or different community and/or environment than the intended host or environment of application. The general concept of phage local adaptation, where phages are found to be more infective to their local host populations than "foreign" ones, has been well described and demonstrated across systems (59–66). In our immature pear fruit, we did not observe a significant difference in the efficiency of the phage to mitigate symptom development in immature fruit, suggesting that phage 16Q is equally well controlling the two strains collected from Callery pear.

Conclusion

We show that ornamental pear trees function as reservoirs for blossom blight caused by Pss. These strains are characterized by their own unique effector repertoire, arming the bacteria with the virulence factors necessary to infect commercial pear as demonstrated by our immature pear assay. Hence, we conclude that these ornamental pear trees pose a potential risk of inducing spillovers in urban environments expanding to gardens and commercial orchards, creating a potential biological hazard. Future work should focus on the spread of these pathogens in urban environments and include nearby spillover hosts. In our research, we show the promise of phages as biocontrol to mitigate disease, as our newly described 16Q phage reduced symptoms in immature pear fruit across both Pss strains tested. In future research, we should emphasize on the potential of phages to reduce these spillover effects and control the outbreak of disease within urban environments. As we continue to uncover the diversity of circulating pathogens and their associated phages, we can move closer to an integrated disease management strategy that takes into account other host reservoirs and alternatives to chemical controls.

ACKNOWLEDGMENTS

The authors would like to thank Prof. S.E. Lindow for his input and guidance and Ms. J.K. Sherman for her technical assistance.

This research was funded by the NSF and USDA/NIFA Career Award (NSF # 1942881, USDA/NIFA # 1024053). D.H. holds a doctoral fellowship from the "Fonds voor Wetenschappelijk Onderzoek Vlaanderen" (FWO) strategic basic research grant 1S02520N, S.Z.A. is an NSF REPS Fellow, and B.K. is a Chan Zuckerburg San Francisco BioHub investigator.

AUTHOR AFFILIATIONS

[1]Integrative Biology University of California, Berkeley, California, USA
[2]Chan Zuckerberg Biohub, San Francisco, California, USA

AUTHOR ORCIDs

D. Holtappels http://orcid.org/0000-0003-4263-3407

FUNDING

Funder	Grant(s)	Author(s)
National Science Foundation (NSF)	1942881	B. Koskella
USDA | National Institute of Food and Agriculture (NIFA)	1024053	B. Koskella
Fonds Wetenschappelijk Onderzoek (FWO)	1S02520N	D. Holtappels
Chan Zuckerberg Initiative (CZI)		B. Koskella

AUTHOR CONTRIBUTIONS

D. Holtappels, Conceptualization, Formal analysis, Investigation, Methodology, Supervision, Writing – original draft | S. A. Abelson, Investigation, Methodology, Validation, Writing – original draft | S. C. Nouth, Investigation, Methodology, Writing – original draft | G. E. J. Rickus, Investigation, Methodology, Visualization, Writing – original draft | S. Z. Amare, Investigation, Methodology, Writing – original draft | J. P. Giller, Conceptualization, Funding acquisition, Investigation, Methodology, Project administration, Supervision, Writing – original draft, Writing – review and editing | D. Z. Jian, Formal analysis, Investigation, Methodology, Writing – original draft | B. Koskella, Conceptualization, Formal analysis, Funding acquisition, Investigation, Methodology, Project administration, Supervision, Writing – original draft, Writing – review and editing

DATA AVAILABILITY

Draft bacterial genomes are available under NCBI accession numbers SAMN35531629 and PRJNA977714 (for Pss11.5) and SAMN35531935 and PRJNA977718 (for Pss16QsV). The phage genome is accessible under the NCBI accession number OR001909.

ADDITIONAL FILES

The following material is available online.

Supplemental Material

Supplementary figures (Spectrum02833-23-s0001.pdf). All supplementary figures.
Table S1 (Spectrum02833-23-s0002.csv). List of isolates used in this study.
Table S2 (Spectrum02833-23-s0003.csv). fastANI analysis of the isolates used in this study.

REFERENCES

1. Gutiérrez-Barranquero JA, Cazorla FM, de Vicente A. 2019. *Pseudomonas syringae* pv. *syringae* associated with mango trees, a particular pathogen within the "hodgepodge" of the *Pseudomonas syringae* complex. Front Plant Sci 10. https://doi.org/10.3389/fpls.2019.00570
2. Morris CE, Lamichhane JR, Nikolić I, Stanković S, Moury B. 2019. The overlapping continuum of host range among strains in the *Pseudomonas syringae* complex. Phytopathol Res 1:1–16. https://doi.org/10.1186/s42483-018-0010-6
3. Gutiérrez-Barranquero JA, Carrión VJ, Murillo J, Arrebola E, Arnold DL, Cazorla FM, de Vicente A. 2013. A *Pseudomonas syringae* diversity survey reveals a differentiated phylotype of the pathovar syringae associated with the mango host and mangotoxin production. Phytopathology 103:1115–1129. https://doi.org/10.1094/PHYTO-04-13-0093-R
4. Little EL, Bostock RM, Kirkpatrick BC. 1998. Genetic characterization of *Pseudomonas syringae* pv. *syringae* strains from stone fruits in California. Appl Environ Microbiol 64:3818–3823. https://doi.org/10.1128/AEM.64.10.3818-3823.1998
5. Oueslati M, Holtappels D, Fortuna KJ, Hajlaoui MR, Lavigne R, Sadfi-Zouaoui N, Wagemans J. 2022. Biological and molecular characterization of the lytic bacteriophage SoKa against *Pseudomonas syringae* pv. *syringae*, causal agent of citrus blast and black pit in Tunisia. Viruses 14:1–16. https://doi.org/10.3390/v14091949
6. Rabiey M, Roy SR, Holtappels D, Franceschetti L, Quilty BJ, Creeth R, Sundin GW, Wagemans J, Lavigne R, Jackson RW. 2020. Phage biocontrol to combat *Pseudomonas syringae* pathogens causing disease in cherry. Microb Biotechnol 13:1428–1445. https://doi.org/10.1111/1751-7915.13585
7. Spotts RA. 1995. Copper, oxytetracycline, and streptomycin resistance of *Pseudomonas syringae* pv *syringae* strains from pear orchards in Oregon and Washington. Plant Dis 79:1132. https://doi.org/10.1094/PD-79-1132
8. Cazorla FM, Arrebola E, Sesma A, Pérez-García A, Codina JC, Murillo J, de Vicente A. 2002. Copper resistance in *Pseudomonas syringae* strains isolated from mango is encoded mainly by plasmids. Phytopathol 92:909–916. https://doi.org/10.1094/PHYTO.2002.92.8.909
9. Whitesides SK. 1991. Frequency, distribution, and characteristics of endophytic *Pseudomonas syringae* in pear trees. Phytopathology 81:453. https://doi.org/10.1094/Phyto-81-453
10. Barker BTP, Grove O. 1914. A bacterial disease of fruit blossom. Ann Appl Biol 1:85–97. https://doi.org/10.1111/j.1744-7348.1914.tb05413.x
11. Panagopoulos CG, Crosse JE. 1964. Blossom blight and related symptoms caused by *Pseudomonas syringae* van hall on pear trees, p 119–122. In Annals reporter east mailling research statement Kent. Vol. 47.
12. Wilson EE. 1936. Symptomatic and etiologic relations of the canker and the blossom blast of *Pyrus* and the bacterial canker of *Prunus*. Hilg 10:213–240. https://doi.org/10.3733/hilg.v10n08p213
13. Moragrega C, Llorente I, Manceau C, Montesinos E. 2003. Susceptibility of European pear cultivars to *Pseudomonas syringae pv. syringae* using immature fruit and detached leaf assays. Eur J Plant Pathol 109:319–326. https://doi.org/10.1023/A:1023574219069
14. Malvick DK, Moore LW. 1988. Population dynamics and diversity of *Pseudomonas syringae* on maple and pear trees and associated grasses. Phytopathology 78:1366. https://doi.org/10.1094/Phyto-78-1366
15. Sohn KH, Jones JDG, Studholme DJ. 2012. Draft genome sequence of *Pseudomonas syringae* pathovar syringae strain FF5, causal agent of stem tip dieback disease on ornamental pear. J Bacteriol 194:3733–3734. https://doi.org/10.1128/JB.00567-12
16. Holtappels D, Lavigne R, Huys I, Wagemans J, Holtappels D, Lavigne R, Huys I, Wagemans J. 2019. Protection of phage applications in crop production: a patent landscape. Viruses 11:1–16. https://doi.org/10.3390/v11030277
17. Pinheiro LAM, Pereira C, Frazão C, Balcão VM, Almeida A. 2019. Efficiency of phage Φ6 for biocontrol of *Pseudomonas syringae* pv *syringae*: an *in vitro* preliminary study. Microorganisms 7:286. https://doi.org/10.3390/microorganisms7090286

18. Akbaba M, Ozaktan H. 2021. Evaluation of bacteriophages in the biocontrol of *Pseudomonas syringae* pv. *syringae* isolated from cankers on sweet cherry (*Prunus avium L.*) in Turkey. Egypt J Biol Pest Control 31:1–11. https://doi.org/10.1186/s41938-021-00385-7
19. Arroyo-Velez N, González-Fuente M, Peeters N, Lauber E, Noël LD. 2020. From effectors to effectomes: are functional studies of individual effectors enough to decipher plant pathogen infectious strategies. PLoS Pathog 16:e1009059. https://doi.org/10.1371/journal.ppat.1009059
20. Beer SV, Rundle JR. 1983. Suppression of *Erwinia amylovora* by erwinia herbicola in immature pear fruits. Phytopathology 73:1346. https://doi.org/10.1094/Phyto-73-1328
21. Kim WS, Hildebrand M, Jock S, Geider K. 2001. Molecular comparison of pathogenic bacteria from pear trees in Japan and the fire blight pathogen *Erwinia amylovora*. Microbiology 147:2951–2959. https://doi.org/10.1099/00221287-147-11-2951
22. Yessad S, Manceau C, Luisetti J. 1992. A detached leaf assay to evaluate virulence and pathogenicity of strains of *Pseudomonas syringae* pv. *syringae* on pear. Plant Dis 76:370. https://doi.org/10.1094/PD-76-0370
23. Bolger AM, Lohse M, Usadel B. 2014. Trimmomatic: a flexible trimmer for Illumina sequence data. Bioinformatics 30:2114–2120. https://doi.org/10.1093/bioinformatics/btu170
24. Wick RR, Judd LM, Gorrie CL, Holt KE. 2017. Unicycler: resolving bacterial genome assemblies from short and long sequencing reads. PLoS Comput Biol 13:e1005595. https://doi.org/10.1371/journal.pcbi.1005595
25. Seemann T. 2014. Prokka: rapid prokaryotic genome annotation. Bioinformatics 30:2068–2069. https://doi.org/10.1093/bioinformatics/btu153
26. Kumar S, Stecher G, Li M, Knyaz C, Tamura K. 2018. MEGA X: molecular evolutionary genetics analysis across computing platforms. Mol Biol Evol 35:1547–1549. https://doi.org/10.1093/molbev/msy096
27. Letunic I, Bork P. 2021. Interactive tree of life (iTOL) V5: an online tool for phylogenetic tree display and annotation. Nucleic Acids Res 49:W293–W296. https://doi.org/10.1093/nar/gkab301
28. Jain C, Rodriguez-R LM, Phillippy AM, Konstantinidis KT, Aluru S. 2018. High throughput ANI analysis of 90K prokaryotic genomes reveals clear species boundaries. Nat Commun 9:5114. https://doi.org/10.1038/s41467-018-07641-9
29. Gautreau G, Bazin A, Gachet M, Planel R, Burlot L, Dubois M, Perrin A, Médigue C, Calteau A, Cruveiller S, Matias C, Ambroise C, Rocha EPC, Vallenet D. 2020. PPanGGOLiN: depicting microbial diversity via a partitioned pangenome graph. PLoS Comput Biol 16:e1007732. https://doi.org/10.1371/journal.pcbi.1007732
30. Price MN, Dehal PS, Arkin AP. 2009. Fasttree: computing large minimum evolution trees with profiles instead of a distance matrix. Mol Biol Evol 26:1641–1650. https://doi.org/10.1093/molbev/msp077
31. Dillon MM, Almeida RND, Laflamme B, Martel A, Weir BS, Desveaux D, Guttman DS. 2019. Molecular evolution of *Pseudomonas syringae* type III secreted effector proteins. Front Plant Sci 10:418. https://doi.org/10.3389/fpls.2019.00418
32. Hyman P, Abedon ST. 2009. Practical methods for determining phage growth parameters, p 175–202. In Clokie MR, Kropinski AM (ed), Bacteriophages. Methods in molecular biology. Humana Press.
33. Wattam AR, Davis JJ, Assaf R, Boisvert S, Brettin T, Bun C, Conrad N, Dietrich EM, Disz T, Gabbard JL, et al. 2017. Improvements to PATRIC, the all-bacterial bioinformatics database and analysis resource center. Nucleic Acids Res 45:D535–D542. https://doi.org/10.1093/nar/gkw1017
34. Nishimura Y, Yoshida T, Kuronishi M, Uehara H, Ogata H, Goto S. 2017. ViPTree: the viral proteomic tree server. Bioinformatics 33:2379–2380. https://doi.org/10.1093/bioinformatics/btx157
35. Moraru C, Varsani A, Kropinski AM. 2020. VIRIDIC—a novel tool to calculate the intergenomic similarities of prokaryote-infecting viruses. Viruses 12:1–10. https://doi.org/10.3390/v12111268
36. Sullivan MJ, Petty NK, Beatson SA. 2011. Easyfig: a genome comparison visualizer. Bioinformatics 27:1009–1010. https://doi.org/10.1093/bioinformatics/btr039
37. Zhao Y, Blumer SE, Sundin GW. 2005. Identification of *Erwinia amylovora* genes induced during infection of immature pear tissue. J Bacteriol 187:8088–8103. https://doi.org/10.1128/JB.187.23.8088-8103.2005
38. Schindelin J, Arganda-Carrera I, Frise E, Verena K, Mark L, Tobias P, Stephan P, Curtis R, Stephan S, Benjamin S, Jean-Yves T, Daniel JW, Volker H, Kevin E, Pavel T, Albert C. 2009. Fiji - an open platform for biological image analysis. Nat Methods 9:1–15.
39. Nowell RW, Laue BE, Sharp PM, Green S. 2016. Comparative genomics reveals genes significantly associated with woody hosts in the plant pathogen *Pseudomonas syringae*. Mol Plant Pathol 17:1409–1424. https://doi.org/10.1111/mpp.12423
40. Peters SL, Borges AL, Giannone RJ, Morowitz MJ, Banfield JF, Hettich RL. 2022. Experimental validation that human microbiome phages use alternative genetic coding. Nat Commun 13:5710. https://doi.org/10.1038/s41467-022-32979-6
41. Turner D, Kropinski AM, Adriaenssens EM. 2021. A roadmap for genome-based phage taxonomy. Viruses 13:1–10. https://doi.org/10.3390/v13030506
42. Rombouts S, Volckaert A, Venneman S, Declercq B, Vandenheuvel D, Allonsius CN, Van Malderghem C, Jang HB, Briers Y, Noben JP, Klumpp J, Van Vaerenbergh J, Maes M, Lavigne R. 2016. Characterization of novel bacteriophages for biocontrol of bacterial blight in leek caused by *Pseudomonas Syringae* pv. porri. Front Microbiol 7:279. https://doi.org/10.3389/fmicb.2016.00279
43. Almeida RND, Greenberg M, Bundalovic-Torma C, Martel A, Wang PW, Middleton MA, Chatterton S, Desveaux D, Guttman DS. 2022. Predictive modeling of *Pseudomonas syringae* virulence on bean using gradient boosted decision trees. PLoS Pathog 18:e1010716. https://doi.org/10.1371/journal.ppat.1010716
44. Ranković T, Nikolić I, Berić T, Popović T, Lozo J, Medić O, Stanković S. 2023. Genome analysis of two *Pseudomonas syringae* pv. aptata strains with different virulence capacity Isolated from sugar beet: features of successful pathogenicity in the phyllosphere microbiome. Microbiol Spectr 11:e0359822. https://doi.org/10.1128/spectrum.03598-22
45. Dillon MM, Thakur S, Almeida RND, Wang PW, Weir BS, Guttman DS. 2019. Recombination of ecologically and evolutionarily significant loci maintains genetic cohesion in the *Pseudomonas syringae* species complex 06 biological sciences 0604 genetics 06 biological sciences 0603 evolutionary biology. Genome Biol 20. https://doi.org/10.1186/s13059-018-1606-y
46. Bundalovic-Torma C, Lonjon F, Desveaux D, Guttman DS. 2022. Diversity, evolution, and function of *Pseudomonas syringae* effectoromes. Annu Rev Phytopathol 60:211–236. https://doi.org/10.1146/annurev-phyto-021621-121935
47. Lovelace AH, Dorhmi S, Hulin MT, Li Y, Mansfield JW, Ma W. 2023. Effector identification in plant pathogens. Phytopathology 113:637–650. https://doi.org/10.1094/PHYTO-09-22-0337-KD
48. Alfano JR, Charkowski AO, Deng W-L, Badel JL, Petnicki-Ocwieja T, van Dijk K, Collmer A. 2000. The *Pseudomonas syringae* Hrp pathogenicity island has a tripartite mosaic structure composed of a cluster of type III secretion genes bounded by exchangeable effector and conserved effector loci that contribute to parasitic fitness and pathogenicity in plants. Proc Natl Acad Sci U S A 97:4856–4861. https://doi.org/10.1073/pnas.97.9.4856
49. Bundalovic-Torma C, Desveaux D, Guttman DS. 2022. RecPD: a recombination-aware measure of phylogenetic diversity. PLoS Comput Biol 18:e1009899. https://doi.org/10.1371/journal.pcbi.1009899
50. Arnold DL, Jackson RW. 2011. Bacterial genomes: evolution of pathogenicity. Curr Opin Plant Biol 14:385–391. https://doi.org/10.1016/j.pbi.2011.03.001
51. Hulin MT, Armitage AD, Vicente JG, Holub EB, Baxter L, Bates HJ, Mansfield JW, Jackson RW, Harrison RJ. 2018. Comparative genomics of *Pseudomonas syringae* reveals convergent gene gain and loss associated with specialization onto cherry (*Prunus avium*). New Phytol 219:672–696. https://doi.org/10.1111/nph.15182
52. Howard-Varona C, Hargreaves KR, Solonenko NE, Markillie LM, White RA, Brewer HM, Ansong C, Orr G, Adkins JN, Sullivan MB. 2018. Multiple mechanisms drive phage infection efficiency in nearly identical hosts. ISME J 12:1605–1618. https://doi.org/10.1038/s41396-018-0099-8
53. Holtappels D, Alfenas-Zerbini P, Koskella B. 2023. Drivers and consequences of bacteriophage host range. FEMS Microbiol Rev 47:fuad038. https://doi.org/10.1093/femsre/fuad038
54. Silby MW, Winstanley C, Godfrey SAC, Levy SB, Jackson RW. 2011. Pseudomonas genomes: diverse and adaptable. FEMS Microbiol Rev 35:652–680. https://doi.org/10.1111/j.1574-6976.2011.00269.x

55. Frampton RA, Taylor C, Holguín Moreno AV, Visnovsky SB, Petty NK, Pitman AR, Fineran PC. 2014. Identification of bacteriophages for biocontrol of the kiwifruit canker phytopathogen *Pseudomonas syringae* pv. actinidiae. Appl Environ Microbiol 80:2216–2228. https://doi.org/10.1128/AEM.00062-14
56. Warring SL, Malone LM, Jayaraman J, Easingwood RA, Rigano LA, Frampton RA, Visnovsky SB, Addison SM, Hernandez L, Pitman AR, Lopez Acedo E, Kleffmann T, Templeton MD, Bostina M, Fineran PC. 2022. A lipopolysaccharide-dependent phage infects a pseudomonad phytopathogen and can evolve to evade phage resistance. Environ Microbiol 24:4834–4852. https://doi.org/10.1111/1462-2920.16106
57. Holtappels D, Fortuna K, Lavigne R, Wagemans J. 2021. The future of phage biocontrol in integrated plant protection for sustainable crop production. Curr Opin Biotechnol 68:60–71. https://doi.org/10.1016/j.copbio.2020.08.016
58. Wagemans J, Holtappels D, Vainio E, Rabiey M, Marzachì C, Herrero S, Ravanbakhsh M, Tebbe CC, Ogliastro M, Ayllón MA, Turina M. 2022. Going viral: virus-based biological control agents for plant protection. Annu Rev Phytopathol 60:21–42. https://doi.org/10.1146/annurev-phyto-021621-114208
59. Piel D, Bruto M, Labreuche Y, Blanquart F, Goudenège D, Barcia-Cruz R, Chenivesse S, Le Panse S, James A, Dubert J, Petton B, Lieberman E, Wegner KM, Hussain FA, Kauffman KM, Polz MF, Bikard D, Gandon S, Rocha EPC, Le Roux F. 2022. Phage–host coevolution in natural populations. Nat Microbiol 7:1075–1086. https://doi.org/10.1038/s41564-022-01157-1
60. Van Cauwenberghe J, Santamaría RI, Bustos P, Juárez S, Ducci MA, Fleming TF, Etcheverry AV, González V. 2021. Spatial patterns in phage-*Rhizobium* coevolutionary interactions across regions of common bean domestication. ISME J 15:2092–2106. https://doi.org/10.1038/s41396-021-00963-5
61. Scanlan PD, Hall AR, Buckling A. 2017. Parasite genetic distance and local adaptation in co-evolving bacteria–bacteriophage populations. Mol Ecol 26:1747–1755. https://doi.org/10.1111/mec.13897
62. Lopez Pascua L, Gandon S, Buckling A. 2012. Abiotic heterogeneity drives parasite local adaptation in coevolving bacteria and phages. J Evol Biol 25:187–195. https://doi.org/10.1111/j.1420-9101.2011.02416.x
63. Koskella B, Parr N. 2015. . The evolution of bacterial resistance against bacteriophages in the horse chestnut phyllosphere is general across both space and time. Philos Trans R Soc Lond B Biol Sci 370:20140297. https://doi.org/10.1098/rstb.2014.0297
64. Morley D, Broniewski JM, Westra ER, Buckling A, van Houte S. 2017. Host diversity limits the evolution of parasite local adaptation. Mol Ecol 26:1756–1763. https://doi.org/10.1111/mec.13917
65. Vos M, Birkett PJ, Birch E, Griffiths RI, Buckling A. 2009. Local adaptation of bacteriophages to their bacterial hosts in soil. Science 325:833. https://doi.org/10.1126/science.1174173
66. Dewald-Wang EA, Parr N, Tiley K, Lee A, Koskella B. 2022. Multiyear time-shift study of bacteria and phage dynamics in the phyllosphere. Am Nat 199:126–140. https://doi.org/10.1086/717181